Comprehensive quantum chemical analysis of the (ro)vibrational spectrum of thiirane and its deuterated isotopologue

John De Vos[c,a], Benjamin Schröder[b], Guntram Rauhut[a,*]

[a] *Institute for Theoretical Chemistry, University of Stuttgart, Pfaffenwaldring 55, 70569, Stuttgart, Germany*
[b] *Institute for Physical Chemistry, University of Göttingen, Tammannstr. 6, 37077, Göttingen, Germany*
[c] *Department of Chemistry, Ghent University, Krijgslaan 281, 9000, Ghent, Belgium*

Abstract

The (ro)vibrational spectra of thiirane, c-C_2H_4S, and its fully deuterated isotopologue, c-C_2D_4S, have been studied by means of vibrational configuration interaction theory, VCI, its incremental variant, iVCI, and subsequent variational rovibrational calculations, RVCI, which rely on multidimensional potential energy surfaces of coupled-cluster quality including up to four-mode coupling terms. Accurate geometrical parameters, fundamental vibrational transitions and first overtones, rovibrational spectra and rotational spectroscopic constants have been determined from these calculations and were compared with experimental results whenever available. A number of tentative misassignments in the vibrational spectra could be resolved and most results for the deuterated thiirane are high-level predictions, which may guide experiments to come. Besides this, a new implementation of infrared intensities within the iVCI framework has been tested for the transitions of the title compounds and are compared with results obtained from standard VCI calculations.

Keywords: Thiirane, Vibrational configuration interaction theory, Rovibrational calculations, Spectroscopic constants

---

1. Introduction

Thiirane (c-C_2H_4S) is primarily known as the sulfur analog of oxirane (ethylene oxide; [1, 2]) and has been studied by spectroscopic methods since very many years [3–16]. In 1940, Thompson and Dupré [3] performed already a first Raman and mid-infrared (mid-IR) study on thiirane, allowing them to assign 14 out of the 15 fundamental vibrations. Using a spectrometer with increased resolving power, Thompson and Cave [4] were later able to suggest a reassignment of some vibrations. Simultaneously, Guthrie *et al.* studied the IR spectrum of liquid thiirane [6]. The fundamental vibrational transitions as well as some low lying overtones and combination band of both gaseous [8, 9, 11] and liquid thiirane [7, 8] have been revisited by several authors over the years. Allen *et al.* [12] performed a comprehensive study through both low resolution ($\sim$ 1 cm^{-1}) experimental IR and Raman spectra and *ab initio* calculations at the Hartree-Fock level of theory, employing various basis sets. Bane *et al.* [15] revisited the IR spectrum of thiirane by recording high-resolution ($\sim$ 0.0017 cm^{-1}) data for the ν_5 and ν_{12} modes of thiirane in the far-IR region, using the far-IR beamline at the Australian synchrotron. Evans *et al.* [16] expanded on this work to the mid-IR region by recording high-resolution spectra for the ν_4, ν_8, ν_{11}, ν_{14} and ν_{15} fundamental modes. These high-resolution studies serve as a reference for our calculations.

Cunningham *et al.* [5] measured the first microwave spectra of both thiirane and its deuterated isotopologue and used this data to determine the molecular structure and dipole moments. Microwave spectroscopy was also used later by Okiye *et al.* [10] to investigate the rotational structure of the vibrational ground state. In the early 2000s, Hirao *et al.* [14] revisited the ground state and determined millimeter-wave spectra for

---

[*] Corresponding author

Email addresses: `john.devos@ugent.be` (John De Vos), `bschroe4@gwdg.de` (Benjamin Schröder), `rauhut@theochem.uni-stuttgart.de` (Guntram Rauhut)

Preprint submitted to Elsevier *February 7, 2024*

thiirane and a number of isotopomers. Finally, Hirose *et al.* [11] performed a comprehensive study of the rotational spectrum of thiirane in the ground state and five low-lying excited states.

Besides laboratory spectroscopic work thiirane is also known for the fact that it has not yet been observed in the interstellar medium, in contrast to oxirane, which has been detected in astrophysical studies [17]. Although sulfur is one of the most abundant elements in the interstellar medium, the sulfur content detectable in molecular clouds accounts for only ∼0.1% observed in star-forming regions [18, 19]. Hypotheses explaining this "missing" sulfur involve hidden sinks such as ices, dust grains, as well as yet unknown molecular species [20]. Since thiirane is further considered a precursor of prebiotic organosulfur compounds [21], there is considerable interest and the hunt for this particular molecule as well as other sulfur species is ongoing [22–24]. From this point of view it is quite surprising that high-level quantum-chemical studies of the (ro)vibrational spectrum beyond the harmonic approximation are still missing. Besides that, we are not aware of any rovibrational experimental or theoretical studies of the fully deuterated analog. With this study we try to fill this gap and present *ab initio* calculations for both systems.

The accurate quantum chemical calculation of molecular rovibrational spectra is a challenging task and usually faces two bottlenecks, the first one being the determination of the multidimensional potential energy surface (PES) and the second one being the solution of the nuclear Schrödinger equation. In contrast to most applications in electronic structure theory, it is the occurrence of a multitude of resonances caused by the high state density, which puts an extra burden on the latter aspect. Many methods have been developed to solve these problems. Within the time-independent framework 2nd order vibrational perturbation theory (VPT2) is widely used to calculate spectra beyond the harmonic approximation [25–32]. However, this approach relies on a truncated representation of the PES, i.e. a quartic force field, which limits the applicability of the method to low-lying states. Due to the underlying perturbational expansion it is frequently plagued by issues arising from resonances which require a special treatment [27, 33]. Whether a resonance needs to be accounted for already requires detailed knowledge of the PES and black-box type implementations of VPT2 which automatically detect and account for necessary resonances are still a topic of current research [34–41]. Comparably more flexible are variational approaches as for example vibrational configuration interaction (VCI) theory [42, 43]. However, these go along with higher computational demands, which limit their applicability.

In order to exploit the advantages of modern multicore architectures, we have introduced incremental vibrational configuration interaction theory (iVCI) quite recently, in which the vibrational state energy is represented in terms of a many-body expansion. This allows to distribute the individual increments within this expansion among the available cores. For details on configuration-selective iVCI see Refs. [43–45]. Our implementation of iVCI theory was restricted to the calculation of vibrational state energies, which are just one half of the information needed for the simulation of an IR spectrum. The other half is given by the corresponding intensities. In order to retrieve the vibrational wavefunction, which is needed for the calculation of the transition moments, an additional diagonalization at the end of a state-specific iVCI calcultion was introduced, which readily provides the needed information. However, since this diagonalization is done in the space of all selected configurations it destroys the performance and the overall philosophy behind iVCI theory. For that very reason, we have augmented iVCI theory by a many-body expansion of the transition dipole moments as needed for the simulation of IR spectra. In addition to the analysis of thiirane this study provides the first benchmark for the new implementation of IR intensities within iVCI.

The integrated absorption coefficient can be written as

$$I = \frac{2\pi^2}{3}\frac{N_\mathrm{A}}{\epsilon_0 h^2 c^2}\left|\langle\Psi_r\left|\boldsymbol{\mu}\right|\Psi_f\rangle\right|^2 \Delta E_{rf}\Delta n(T) \qquad (1)$$

with Ψ_r denoting the vibrational wavefunction of the reference state, e.g. the vibrational ground state, Ψ_f the corresponding wavefunction of the final state and $\boldsymbol{\mu}$ is the dipole moment surface with Cartesian components μ_α. ΔE_{rf} is the transition energy as evaluated from the many-body expansion and $\Delta n(T)$ takes account of the temperature dependence, i.e. the occupation of the rovibrational states. In the limit $T \longrightarrow 0$ this factor will be 1. In principle, the components of the transition dipole moment vector $D^\alpha_{rf} = \langle\Psi_r\left|\mu_\alpha\right|\Psi_f\rangle$ can be expanded as

$$D^{\alpha}_{rf} = \left(D^{\alpha}_{rf}\right)_0 + \sum_{i}^{n_{\mathrm{b}}} \Delta \left(D^{\alpha}_{rf}\right)_i + \sum_{i<j}^{n_{\mathrm{b}}} \Delta \left(D^{\alpha}_{rf}\right)_{ij} + \dots \tag{2}$$

Since the individual terms in the last equations can be computed from iVCI eigenvectors of the incremental subspaces, which are needed for the corresponding energy increments, the additional diagonalization at the end of an iVCI calculation can be avoided. This leads to an improvement in performance and the additional memory requests are negligible. As a side aspect of this study we provide a comparison of standard configuration-selective VCI results with the corresponding iVCI solutions for IR intensities.

The VCI wave functions for the individual vibrational states serve as basis functions within the rovibrational configuration interaction calculations, RVCI. RVCI theory is explained in detail in Refs. [46, 47] and benchmark calculations with respect to the expansion of the individual terms of the underlying Watson Hamiltonian [48] are provided in Ref. [49].

2. Computational Details

All-electron explicitly correlated coupled-cluster theory [50] accounting for single and double excitations and a perturbative treatment of the triple excitations, i.e. CCSD(T)-F12a/cc-pCVTZ-F12 [51], has been used to determine the geometry, harmonic frequencies and the normal coordinates of the molecule and its fully deuterated isotopologue. Auxiliary aug-cc-pVTZ/JKFIT and cc-pCVTZ/MP2FIT basis set was used for density fitting [52–54], and an cc-pCVTZ-F12/OPTRI basis for the resolution of the identity (RI) approximation [51]. The different exponents γ of the Slater geminal functions for the core-core, core-valence and valence-valence orbital pair values were set to 0.8, 1.7 and 2.2, respectively [55]. The complementary auxiliary basis set correction (CABS) has been used to improve the Hartree–Fock energies [56].

The molecule was oriented according to the I^r convention. An n-mode expansion [42] being truncated after the 4-mode coupling terms was used for representing the multidimensional potential energy surfaces (PES). A multi-level scheme [57] was used, in which the 1D and 2D terms of the PES were determined at the same level as the geometry and harmonic frequencies, while the 3D terms were evaluated employing the explicitly correlated distinguishable clusters approximation [58] in combination with a basis set of double-ζ quality, i.e. DCSD-F12a/cc-pCVDZ-F12. The 4D terms were determined by frozen core 2nd order Møller-Plesset perturbation theory, MP2/cc-pVDZ [59, 60] The dipole moment surface has been calculated at the levels of frozen core DCSD/cc-pVTZ-F12 (1D, 2D), DCSD/cc-pVDZ-F12 (3D) and MP2/cc-pVDZ (4D) theory. These surfaces have been transformed to an analytical sum-of-products representation by using Kronecker product fitting [61]. Not more than 8 monomials per mode were needed for both molecules.

State-specific vibrational self-consistent field (VSCF) calculations employing 18 distributed Gaussians per mode were used to determine optimized one-mode wavefunctions (modals) [62, 63]. Vibrational angular momentum terms making use of a constant μ-tensor as occurring in the Watson Hamiltonian for non-linear molecules [48] were included within the VSCF iterations. Subsequent configuration-selective VCI and iVCI calculations were performed state-specifically [64, 65]. The initial correlation space was restricted to sixtuple excitations with respect to the VSCF reference Hartree-product (configuration), a maximal sum of quantum numbers of 12 and a maximal excitation per mode up the 7th root resulting in ca. $8.7 \cdot 10^6$ configurations per irreducible representation (irrep). Vibrational angular momentum terms were accounted for with a constant μ-tensor for all non-diagonal elements of the VCI matrix, but including 1st order terms for the diagonal elements. Within the iVCI calculations resonance corrected mode-based bodies were employed and prescreening of the individual terms of the many-body expansion (the increments) was used in all calculations with default threshold parameters [45]. Within the iVCI calculations of the transition moments, the wave function of the vibrational ground state was not represented by a many-body expansion, but instead was obtained from the eigenvector of a VCI matrix in the basis of all previously selected configurations, i.e. only the excited vibrational state is represented by a many body expansion.

Within the subsequent RVCI calculations, a

Table 1: Geometrical parameters (bondlengths in Å and angles in degrees) of thiirane and its deuterated isotopologue.

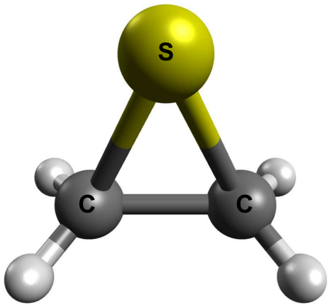

		c-C_2H_4S			c-C_2D_4S	
	$\mathbf{r}_e$	$\mathbf{r}_a$	$\mathbf{r}_g$	$\mathbf{r}_0$ [a]	$\mathbf{r}_a$	$\mathbf{r}_g$
r(CS)	1.8093	1.8173	1.8177	1.8174	1.8167	1.8173
r(CC)	1.4808	1.4894	1.4907	1.4840	1.4885	1.4900
r(CH)	1.0800	1.0863	1.1012	1.0852	1.0850	1.0955
∠(CSC)	48.31	48.38		48.19	48.37	
∠(HCC)	117.93	118.00			117.98	
∠(HCS)	115.06	115.07			115.04	

[a] Experimental data obtained from millimeter-wave spectra taken from Ref. [14].

maximal angular momentum quantum number of $J_{\max} = 90$ has been chosen, which was found to yield converged spectra. Within the calculation of the rotational terms an n-mode expansion up to 2nd order of the μ-tensor has been used, while the expansion was restricted to 1st order for the Coriolis coupling terms. These choices rely on our recently published benchmark study [49]. A molecule specific rotational basis (MSRB) has been used for describing the rotational contributions of the rovibrational wave functions. For details see Ref. [46]. The vibrational basis consists of 32 VCI state functions for c-C_2H_4S and 48 wave functions for c-C_2D_4S. These include the fundamental transitions, first overtones and combination bands with at most double excitations up to 2000 cm^{-1}. As the rovibrational spectra presented in this work do not exceed 1500 cm^{-1}, this rather limited upper bound was found to be sufficient. Hot bands have not been considered in the RVCI calculations since the lowest excited vibrational state in both isotopologues are well above the thermal energy at 300 K and therefore no significant population of these states is expected.

All calculations have been performed with the MOLPRO package of *ab initio* programs [66].

3. Results and Discussion

3.1. Geometrical Parameters

Geometrical parameters of thiirane and its isotopologue have been determined from geometry optimizations on the Born-Oppenheimer potential energy surface, $\mathbf{r}_e$, and from vibrational averaging, $\mathbf{r}_a$ and $\mathbf{r}_g$. The vibrationally averaged parameters have been obtained from the expectation value of the atomic positions, $\mathbf{r}_a$, or an expansion of the bond lengths in terms of normal coordinates, $\mathbf{r}_g$ [67, 68]. The correlated VCI wave function of the vibrational ground state has been used for averaging in both cases, i.e. temperature effects have been neglected. Similar to the exclusion of hot bands, this approximation appears to be justified as the molecule is fairly rigid and the first excited vibrational state is already quite high in energy. All data are summarized in Table 1.

As must be expected, vibrational averaging, i.e. $\mathbf{r}_a$ as well as $\mathbf{r}_g$ structures, leads to an increase of the corresponding lengths for all different bonds in c-C_2H_4S and c-C_2D_4S compared to the equilibrium structure. Structural parameters for the main isotopologue c-C_2H_4S have also been obtained previously using different experimental techniques [5, 10, 14]. Table 1 provides a comparison of our calculated parameters with the most recent $\mathbf{r}_0$ values of Hirao *et al.* obtained from millimeter-wave spectra [14]. The agreement of our computed $\mathbf{r}_a$ values and the $\mathbf{r}_0$ parameters of Hirao *et al.* is excellent. The largest difference of 0.0054 Å can be seen for the CC bond, which goes along with a slightly smaller CSC angle in comparison to our computed value. For the CS and CH bond lengths the differences between our $\mathbf{r}_a$ structure and the $\mathbf{r}_0$ structure of Hirao *et al.* are 0.0001 and 0.0011 Å, respectively.

3.2. Vibrational Frequencies

A comparison of our computed VCI and iVCI frequencies with experimental data for the fundamental bands and some low lying vibrational overtones of thiirane is provided in Table 2.

Table 2: Computed vibrational transition frequencies [cm^{-1}] and IR band intensities [km/mol] for c-C_2H_4S and comparison to experimental values.

			VCI		iVCI		Exp.			
Sym.	#	Harm.	ν_i	IR	ν_i	IR	Ref. [8]	Ref. [69]	Ref. [12]	Refs. [15, 16]
A_1	ν_1	3145.2	3016.5	14.9	3016.5	14.4		3012	*3013.5*	
	ν_2	1500.8	1456.8	2.0	1456.6	1.9	1456	1454	*1456.8*	
	ν_3	1143.9	1112.9	1.1	1112.7	1.1	1109.5	1109	*1109.9*	
	ν_4	1047.6	1023.5	1.0	1023.5	1.1	1033	1024	1024.0	*1024.2*
	ν_5	648.0	632.6	21.1	632.4	22.8	627.5	624		*628.1*
A_2	ν_6	3231.3	3079.4	0.0	3079.4	0.0		*3088*		
	ν_7	1200.4	1171.2	0.0	1171.0	0.0	1173	*1070*		
	ν_8	906.5	888.8	0.0	888.7	0.0	890	891		*893.9*
B_1	ν_9	3142.9	3013.8	8.0	3014.7	10.2		3012	*3013.5*	
	ν_{10}	1476.5	1435.8	0.9	1435.6	0.9	1435	1434	*1435.9*	
	ν_{11}	1080.0	1051.8	21.1	1051.8	21.1	1050	1050	1050.8	*1051.2*
	ν_{12}	691.3	674.9	0.8	674.7	0.8	668	660		*669.7*
B_2	ν_{13}	3244.1	3092.0	5.9	3092.4	8.7		3088	*3088*	
	ν_{14}	965.5	945.4	2.7	945.3	2.7	944	945	945.2	*945.8*
	ν_{15}	835.7	824.4	0.3	824.3	0.3	824	824	827.3	*825.5*
A_1	$2\nu_2$	3001.6	2903.7	0.5	2902.5	1.8	2904		*2903.6*	
	$2\nu_{10}$	2953.0	2861.8	0.6	2861.8	0.5	2863		*2863.5*	
	$2\nu_7$	2400.8	2338.3	0.0	2338.3	0.0	(2323)^b			
	$2\nu_3$	2287.8	2215.6	0.0	2215.6	0.0				
	$2\nu_{11}$	2160.0	2099.5	0.6	2099.4	0.6	*2098*			
	$2\nu_4$	2095.2	2046.5	0.8	2046.5	0.8	*2041*			
	$2\nu_{14}$	1931.0	1889.4	0.0	1889.2	0.0				
	$2\nu_8$	1813.0	1777.2	0.0	1776.7	0.0	*1771*			
	$2\nu_{15}$	1671.4	1650.9	0.0	1651.9	0.0				
	$2\nu_{12}$	1382.6	1343.4	0.0	1343.1	0.0				
	$2\nu_5$	1296.0	1264.0	0.1	1263.7	0.1			*1255*	
MAD^a		63.4	2.9		3.0					
MAX^a		156.1	9.0		8.7					

^{a} Mean absolute deviation (MAD) and maximum absolute deviation (MAX) with respect to experimental reference data being italicized.

^{b} Excluded from the statistics, see text.

Apparently, the VCI and iVCI results coincide in most cases and the newly implemented incremental determination of the IR intensities works very well. The only slightly larger difference in the transition energies (0.9 cm^{-1}) and the IR intensities (2.2 km/mol) can be seen for the ν_9 band. However, this is a fairly sensitive transition as the 9^1 vibrational state shows a pronounced 1-3 Darling-Dennison resonance with the combination state $4^1 7^1 15^1$, i.e. one band occurs at 3013.8 cm^{-1} (61% 9^1; 21% $4^1 7^1 15^1$) and the other at 3030.3 cm^{-1} (20% 9^1; 66% $4^1 7^1 15^1$). In such a case iVCI has been shown to be very dependent on the employed body definition when combined with prescreening [44]. The employed resonance-corrected bodies have been introduced previously [45] to account for this by combining the modes involved in the resonance into a single body, i.e. for *c*-C_2H_4S a body which comprises the modes 9, 4, 7, 15 thus ensuring that the resonance is treated at the lowest order possible of the many-body expansion. However, the above mentioned 1-3 resonance is not recognized by our detection scheme when constructing the bodies [45] and has thus not been incorporated into the body definition. Prescreening then leads to a different convergence pattern of the many-body expansion and final state energy compared to conventional VCI. Nevertheless, the effect of the resonance is still incorporated into the iVCI result and the absolute difference between VCI and iVCI for ν_9 is still smaller than the MAD when comparing to experimental results (cf. Tab. 2). Despite these small shortcomings, prescreening within iVCI does improve the memory efficiency by reducing the size of the largest initial configuration space that needs to be stored by up to a factor of about 3.

The overall agreement of the computed frequencies with experimental data taken from the literature is excellent. As the compilation of Spiekermann *et al.* [69] is based on the dataset of Hirokawa *et al.* [9], but contains corrections for the A_2 fundamentals, we have listed the refined collection of Spiekermann *et al.* Both, the dataset of Spiekermann *et al.* and that of Allen *et al.* [12] show pairwise identical transition frequencies for the CH stretching modes. In case of the A_2/B_2 pair, the IR inactive fundamental ν_6 occurs at the same frequency as ν_{13} and thus its assignment is tentative. Moreover, Coriolis coupling effects render the accurate assignments of these modes a tedious task. The largest deviation from experimental reference data can be seen for the overtone $2\nu_7$ at 2323 cm^{-1} (Exp.) or 2338.3 cm^{-1} (Calc.). However, according to our calculations this overtone does not show any IR intensity, but has been observed in gas phase IR experiments by Aleksanyan and Kuz'yants [8]. Instead, VCI calculations for the combination band $\nu_8 + \nu_{10}$ provide a transition frequency of 2321 cm^{-1}, which shows weak IR intensity of 0.14 km/mol and which is very close to the experimental transition frequency. Thus, we believe that the band observed by Aleksanyan and Kuz'yants belongs to the $\nu_8 + \nu_{10}$ combination band rather than the $2\nu_7$ overtone. For that reason, this transition has been excluded from the statistics as provided in Table 2.

The maximum deviation for the transitions compiled in Table 2 of 9.0 cm^{-1} is observed for the $2\nu_5$ overtone, but the mean absolute deviation (MAD) is as low as 2.9 cm^{-1}, which is in the typical range of VCI calculations at this level of *ab initio* theory, see Ref. [43]. The only other large deviation of 8.6 cm^{-1} can be seen for the IR inactive ν_6 transition. As discussed above, the experimental value for this transition of 3088 cm^{-1}, which has been listed in the work of Spiekermann *et al.* [69] and was taken from Hirokawa *et al.* [9], is the same as for ν_{13}, which shows a decent intensity. In other words: these authors assume that the IR inactive ν_6 transition would occur at the same frequency as the B_2 ν_{13} band. This assumption had already been made by Thompson and Dupré in 1940, based on a low-resolution Raman spectrum where both bands would be active [3]. However, in our calculation these bands are split by about 13 cm^{-1}, irrespective if harmonic or anharmonic frequencies are considered. This raises some questions about the reliability of the experimental assignment. The most reliable experimental results are those of McNaughton an co-workers [15, 16] from high-resolution measurements, but unfortunately these authors studied only 7 of the 15 fundamental vibrations.

The situation for the fully deuterated thiirane, *c*-C_2D_4S, appears to be even more intricate than for thiirane. The vibrational frequencies for this system are compiled in Table 3. The A_1 fundamental ν_2 shows Fermi resonances with the overtones $2\nu_5$ and $2\nu_{15}$, i.e. three transitions with negligible IR intensity can be seen in the calculations, that is, at 1194.2 cm^{-1} (57% 2^1; 21% 15^2; 18% 5^2), 1243.3 cm^{-1} (21% 2^1; 76% 5^2), and at 1174.7 cm^{-1} (19%

Table 3: Computed vibrational transition frequencies [cm^{-1}] and IR band intensities [km/mol] for *c*-C_2D_4S and comparison to experimental values.

			VCI		iVCI		Exp.	
Sym.	#	Harm.	ν_i	IR	ν_i	IR	Ref. [9]	Ref. [12]
A_1	ν_1	2290.0	2216.0	7.1	2216.0	7.1	2215	*2212.5*
	ν_2	1232.1	1194.2	0.0	1194.4	0.0	(1090)^{b,d}	
	ν_3	962.9	945.1	2.7	945.1	2.7	(1020)^{b,d}	*946.4*
	ν_4	782.9	767.9	0.5	767.9	0.5	767	*766.5*
	ν_5	630.1	617.7	19.6	617.7	19.5	608	*613.3*
A_2	ν_6	2412.5	2329.3	0.0	2329.3	0.0	*2330*	
	ν_7	941.1	925.3	0.0	925.3	0.0	(650)^{b,d}	
	ν_8	653.6	644.1	0.0	644.1	0.0	622^{c,d}	
B_1	ν_9	2271.3	2188.2	4.6	2188.2	4.6	2183	*2185.2*
	ν_{10}	1086.9	1065.0	0.9	1065.0	0.9	1064	*1064.2*
	ν_{11}	853.3	833.7	8.6	833.7	8.6	831	*830.7*
	ν_{12}	652.6	640.7	1.8	640.7	1.8	610^{d}	
B_2	ν_{13}	2416.8	2332.5	2.9	2332.5	2.9	2330	*2331.3*
	ν_{14}	722.3	712.0	0.9	712.2	0.9	710	*710.8*
	ν_{15}	594.8	588.5	0.1	588.5	0.1	575	*578.1*
A_1	$2\nu_2$	2464.2	2411.5	0.0	2411.5	0.0		
	$2\nu_{10}$	2173.8	2123.9	0.3	2124.0	0.1		*2125*
	$2\nu_3$	1925.8	1888.4	0.0	1888.5	0.0		
	$2\nu_7$	1882.2	1848.3	0.0	1848.3	0.0		
	$2\nu_{11}$	1706.6	1661.6	0.3	1661.6	0.3		
	$2\nu_4$	1565.7	1533.2	0.2	1533.2	0.2		
	$2\nu_{14}$	1444.6	1422.9	0.0	1422.8	0.0		
	$2\nu_8$	1307.1	1288.5	0.0	1288.5	0.0		
	$2\nu_{12}$	1305.3	1277.0	0.0	1277.0	0.0		
	$2\nu_5$	1260.1	1243.1	0.0	1243.1	0.0		*1241.3*
	$2\nu_{15}$	1189.6	1174.4	0.0	1174.4	0.0		
MAD^a		40.2	2.6		2.6			
MAX^a		86.1	10.4		10.4			

^{a} Mean absolute deviation (MAD) and maximum absolute deviation (MAX) with respect to experimental reference data being italicized.

^{b} Tentative misassignment, see text.

^{c} Obtained from solid state measurements.

^{d} Excluded from the statistics, see text.

2^1; 75% 15^2). These resonances were also incorporated into the mode-based body definitions and in consequence the differences between iVCI and VCI are marginal, not exceeding 0.2 cm^{-1}. At the same time, the largest initial configuration space, i.e. before selection, was again reduced by up to a factor of about 3 due to prescreening.

At a first glance the agreement of the theoretical results with some of the experimental data appear much worse than for non-deuterated thiirane. This is surprising as from a theoretical point of view there are essentially no arguments why the calculation for the deuterated species should result in a different accuracy than for the non-deuterated molecule. Therefore, upon closer inspection a number of the experimental data have been found to be suspicious and thus need to be excluded from the direct comparison. For example, the two A_1 modes listed by Hirokawa *et al.* [9] at 1090 and 1020 cm^{-1} show deviations of up to 104 cm^{-1} from our calculations and in one case the observed value lies even above the calculated harmonic one. This assignment has been revised by Allen *et al.* [12] and their value is in very nice agreement with our result. According to Hirokawa *et al.* [9] the ν_7 fundamental appears at 650 cm^{-1}, but on the basis of data from Aleksanyan and Kuz'yants [8], Spiekermann [69] provided a reassigned value of 900 cm^{-1}, which, however, is just an estimate. Our value is slightly larger than this approximate value. The modes ν_8 and ν_{12} show deviations of more than 20 cm^{-1} from the computed values, which is far beyond the error bar of the applied VCI methods for such a semi-rigid molecule. These are the lowest modes within their respective irreps and a comparison with the non-deuterated thiirane shows, that these agree nicely with the more reliable data of Allen *et al.* [12], which are unfortunately not available for the deuterated species. In their vapor phase spectrum Hirokawa *et al.* [9] observe the center of a transition at 637 cm^{-1}, which they did not assign. The question arises, if this band belongs to the ν_{12} mode, which would be in nice agreement with our calculations. Due to these imponderables and the fact that the experimental value for the IR inactive ν_8 mode at 622 cm^{-1} is based on solid state measurements, these data have also been excluded from the statistics. Again, the experimental values for the A_2 and B_2 CD stretchings are identical and the IR inactive mode is assumed to occur at the same frequency as the the B_2 mode. Moreover, Hirokawa *et al.* [9] observed a Q branch at 2126 cm^{-1}, which they did not assign. However, this values agrees nicely with the value of Allen *et al.* [12] and our calculated value for the $2\nu_{10}$ overtone.

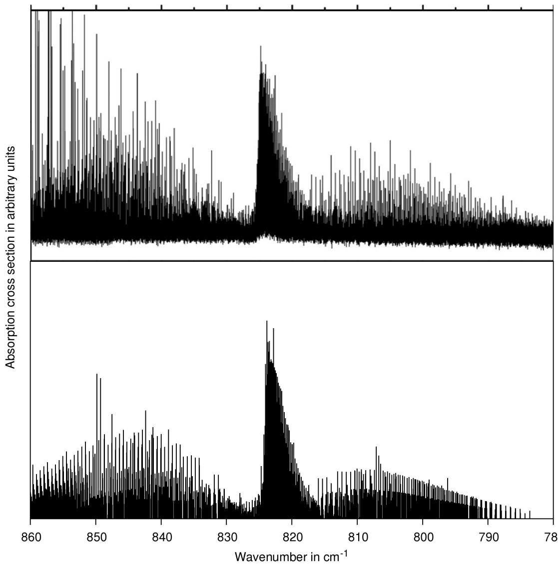

Figure 1: Comparison of the experimental spectrum[1] of Evans *et al.* (upper panel) with our RVCI simulation (lower panel) for the spectral region of the ν_{15} band. A Gaussian line width of 0.0025 cm^{-1} has been used at a temperature of 300 K.

3.3. Rovibrational Spectra

In a first step we compare our simulated rovibrational spectra with the measured ones[1] of Evans *et al.* [16]. Note that, the labeling of the vibrational modes in the papers of Evans *et al.* [16] and Bane *et al.* [15] refers to the II^r representation, while we use the I^r representation, which is also used by most other authors. As a consequence, the irreps and the labeling of the modes of this C_{2v} molecule change. The comparisons are provided in Figs. 1 and 2. The intense lines in the experimental spectra between 860 and 830 cm^{-1} (Fig. 1, upper panel) and at about 950 cm^{-1} (Fig. 2, upper panel) arise, according to Evans *et al.* [16], from ethylene impurities. While the overall appearance of the spectra is nicely represented by the RVCI calculations, e.g. the shape of the Q branches, the individual intensities of the individual rovibrational

---

[1] Reprinted from J. Mol. Spectrosc., 316, C.J. Evans *et al.*, Synchrotron IR spectroscopy of the ν_4, ν_8, ν_{10}, ν_{11} and ν_{14} fundamental bands of thiirane, 32-37, 2015, with permission from Elsevier.

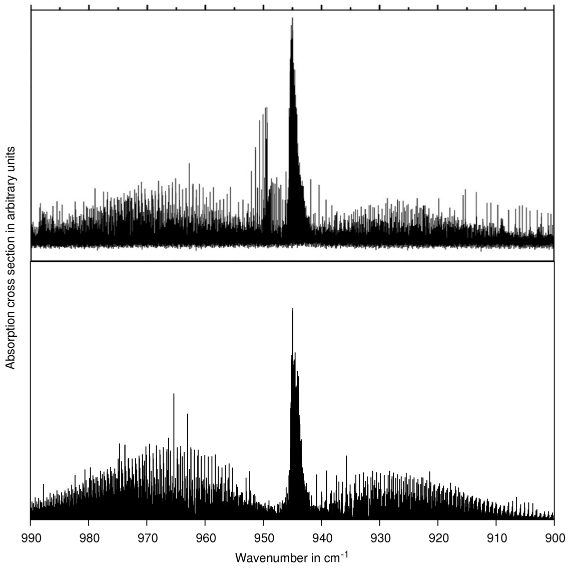

Figure 2: Comparison of the experimental spectrum[1] of Evans *et al.* (upper panel) with our RVCI simulation (lower panel) for the spectral region of the ν_{14} band. A Gaussian line width of 0.0020 cm^{-1} has been used at a temperature of 300 K.

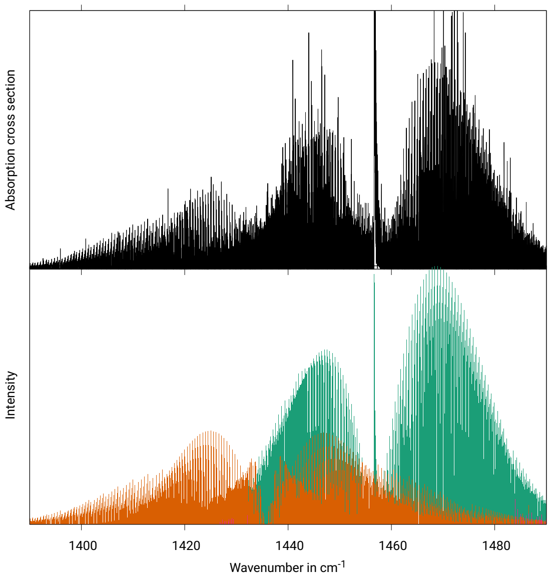

Figure 3: Computed rovibrational spectrum of thiirane in the region between 1390 and 1490 cm^{-1}. Transitions for ν_{10} are shown in orange, those for ν_2 in green. The upper plot includes line broadening effects simulated by Gaussians with a FWHM of 0.002 cm^{-1}.

transition still differ to some extent. This must be expected as the Gaussian envelopes lead to different intensities in dependence on the positions of the transitions, which are very sensitive with respect to the quality of the PES. For that very reason, we will mainly discuss spectra without line broadening effects in the following.

Figure 3 shows the simulated spectral region between 1390 and 1490 cm^{-1}, which has not been investigated in the work of Evans *et al.* [16] or Bane *et al.* [15] and which covers the ν_2 (A_1) and ν_{10} (B_1) transitions. The former shows a *A*-type contour (with the selection rules of $\Delta J = 0, \pm 1$ and $\Delta K_a = 0, \pm 2$, $\Delta K_c = \pm 1$) and the latter a *B*-type contour (with the selection rules of $\Delta J = 0, \pm 1$ and $\Delta K_a = \pm 1$, $\Delta K_c = \pm 1$). Both simulations, i.e. with and without the inclusion of line broadening effects, refer to room temperature (300 K). The color coding of the bands reveals that the R branch of ν_{10} is almost exclusively hidden behind the P branch of the more intense ν_2. Coriolis coupling effects between these two modes are small, which is supported by a value of the corresponding ζ-constant along the *c*-axis of 0.015.

To the best of our knowledge, the high-resolution rovibrational spectrum of c-C_2D_4S has not yet been studied. An overview spectrum between 550 and 1000 cm^{-1} is shown in Fig. 4. This spectral region is the most relevant (cf. Table 3) as the most intense bands are in this region. Another interesting region is that of the CD stretching modes, but this is out of range for our RVCI calculations as it would require the inclusion of very many combination bands, which currently results in an exceeding computational effort. Clearly, most bands are nicely separated and hardly reveal any interactions. However, ν_5 (A_1) at 617.7 cm^{-1} and ν_{12} (B_1) at 640.7 cm^{-1} in fact are coupled, as can be seen from the asymmetry in the P and R branches. This *c*-type Coriolis resonance is also supported by by a ζ-constant of -0.796 for this mode pair. The overlapping branches of these two bands are much weaker than the corresponding outer branches. Based on the band intensities given in Table 3 the ν_{12} borrows intensity from the ν_5 fundamental leading to an *A*-type band shape without the characteristic *Q*-branch, despite ν_{12} nominally being a *B*-type band. Moreover, the typical *B*-type structure for intermediate asymmetry ($\kappa = -0.4476$) can clearly be seen for the ν_{11} band. Finally, the ν_3 band around 945 cm^{-1} exhibits a rather broad *Q*-branch com-

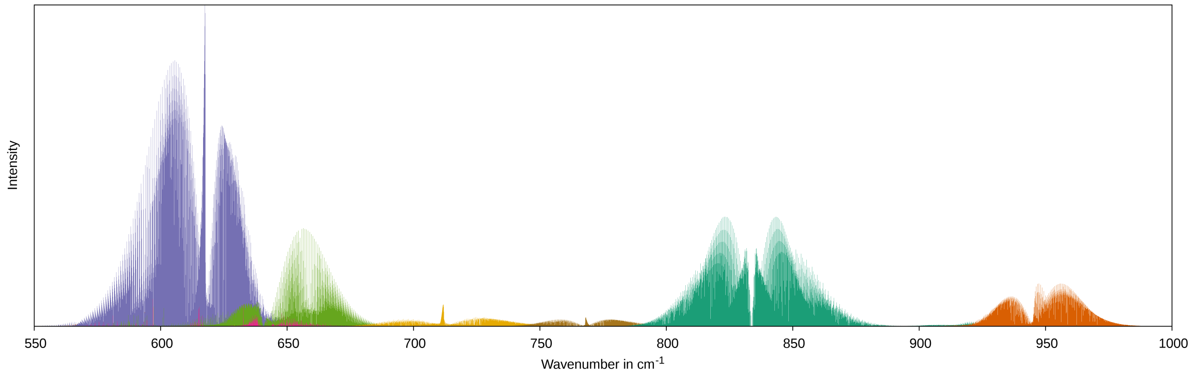

Figure 4: Computed rovibrational spectrum of fully deuterated thiirane without line broadening effects in the region between 550 and 1000 cm^{-1}. Transitions of ν_5 are displayed in purple, of ν_{12} in lightgreen, ν_{14} in yellow, ν_4 in brown, ν_{11} in darkgreen and ν_3 in orange.

pared to other A-type bands depicted in Fig. 4. This could indicate a large change in the A rotational parameter with respect to the vibrational ground state. However, based on VPT2 calculations, the vibration rotation coupling constant α_3^a amounts to about 36 MHz which is comparable to the value of other A-type bands, e.g. for the ν_4 we calculate $\alpha_4^a = 17$ MHz. A closer look at the VPT2 calculations shows that α_3^a has been corrected for an a-type Coriolis resonance with the IR inactive ν_7 ($\zeta_{3,7}^a = -0.511$). The perturbed value of α_3^a amounts to as much as -353 MHz indicating a strong Coriolis resonance which might explains the broad Q-branch.

3.4. Rotational Spectroscopic Constants

Spectroscopic constants are a convenient way to squeeze endless line lists into a very limited number of physically relevant parameters. These can be obtained from fitting the line lists to a model Hamiltonian or from vibrational perturbation theory. Our computed results rely on the latter approach and will be compared with fitted constants obtained from experimental spectra. For thiirane, spectroscopic constants relying on the I^r representation are available for both, Watson's A and S-reduced Hamiltonians [70–73]. While Hirao *et al.* [14] preferred the A-reduction, Evans *et al.* [16] favored the S-reduction. We have computed both sets and the comparisons are shown in Table 4. Note, the force constants being used in our perturbational calculations have not been obtained from numerical differentiation as is typical for quartic force fields [30], but from the polynomial fit of the n-mode representation of the PES [74]. However, usually the differences are negligible. Apparently, our computed values match both parameter sets very well, but the agreement with constants within the A-reduction is slightly better. In particular the deviations in the sextic centrifugal distortion constants are considerably smaller than for the S-reduction, e.g. ϕ_{JK} vs. h_2. Within the A-reduction the average deviation for the rotational constants is 0.1%, for the quartic distortion constants it is 2.6% and 4.2% for the sextic constants. These deviations arise at least partly from missing contributions in the electronic structure calculations employed in the generation of the PES, as for example neglected high-order coupled-cluster terms, relativistic contribution, diagonal Born-Oppenheimer corrections etc., which were out of range within this study here. Nevertheless, the agreement between our equilibrium centrifugal distortion constants obtained from perturbation theory, i.e. without accounting for vibrational averaging, and the experimental vibrational ground state results is a testament to the semi-rigid nature of the title compounds.

The good agreement for the main isotopologue made us confident that the results for the deuterated species, for which no experimental results are available, are of comparable accuracy. The results of these predictions are listed in Table 5. As must be expected, all constants for the fully deuterated isotopologue are smaller in magnitude than for the parent molecule. This renders the determination of the constants from fitting particularly tedious, at

Table 4: Comparison of spectroscopic constants for the vibrational ground state of thiirane using Watson's A and S-reduced Hamiltonians in the I^r representation (1σ uncertainty in parenthesis).

A-reduction				S-reduction			
Parameter		This work	Exp. (Ref. [14])	Parameter		This work	Exp. (Ref. [16])
A_0	[MHz]	21963.88	21973.63006(66)	A_0	[MHz]	21963.88	21973.63495(62)
B_0	[MHz]	10845.35	10824.92431(27)	B_0	[MHz]	10845.35	10824.89248(25)
C_0	[MHz]	8035.87	8026.21768(24)	C_0	[MHz]	8035.87	8026.24744(20)
Δ_J	[kHz]	7.744	7.90770(32)	D_J	[kHz]	6.920	7.05229(43)
Δ_{JK}	[kHz]	8.827	8.6382(18)	D_{JK}	[kHz]	13.776	13.7818(15)
Δ_K	[kHz]	20.171	20.704(11)	D_K	[kHz]	16.048	16.4264(81)
δ_J	[kHz]	2.134	2.192687(96)	d_1	[kHz]	−2.134	−2.192568(70)
δ_K	[kHz]	14.881	15.3817(22)	d_2	[kHz]	−0.412	−0.428857(53)
Φ_J	[Hz]	0.003	0.0(*fixed*)	H_J	[Hz]	0.004	0.00237(16)
Φ_{JK}	[Hz]	−0.095	−0.0988(25)	H_{JK}	[Hz]	−0.188	−0.19909(90)
Φ_{KJ}	[Hz]	0.376	0.3747(85)	H_{KJ}	[Hz]	0.665	0.6967(84)
Φ_K	[Hz]	−0.304	−0.293(49)	H_K	[Hz]	−0.502	−0.516(13)
ϕ_J	[mHz]	1.928	2.043(80)	h_1	[mHz]	1.387	1.238(56)
ϕ_{JK}	[Hz]	−0.054	−0.0589(21)	h_2	[mHz]	−0.631	−0.406(47)
ϕ_K	[Hz]	0.407	0.439(10)	h_3	[mHz]	0.541	0.627(11)

Table 5: Computed spectroscopic constants for the vibrational ground state of deuterated thiirane using Watson's A and S-reduced Hamiltonians in the I^r representation.

A-reduction			S-reduction		
A_0	[MHz]	15464.76	A_0	[MHz]	15464.76
B_0	[MHz]	9211.79	B_0	[MHz]	9211.79
C_0	[MHz]	6825.39	C_0	[MHz]	6825.39
Δ_J	[kHz]	4.893	D_J	[kHz]	4.419
Δ_{JK}	[kHz]	4.451	D_{JK}	[kHz]	7.293
Δ_K	[kHz]	6.191	D_K	[kHz]	3.823
δ_J	[kHz]	1.304	d_1	[kHz]	−1.304
δ_K	[kHz]	5.970	d_2	[kHz]	−0.237
Φ_J	[Hz]	0.002	H_J	[Hz]	0.002
Φ_{JK}	[Hz]	−0.039	H_{JK}	[Hz]	−0.071
Φ_{KJ}	[Hz]	0.145	H_{KJ}	[Hz]	0.237
Φ_K	[Hz]	−0.103	H_K	[Hz]	−0.164
ϕ_J	[mHz]	0.887	h_1	[mHz]	0.650
ϕ_{JK}	[Hz]	−0.021	h_2	[mHz]	−0.480
ϕ_K	[Hz]	0.091	h_3	[mHz]	0.237

least for the sextic centrifugal distortion constants, requiring large values of J as well as K_a and K_c to provide numerically stable results.

In order to facilitate future experimental rovibrational studies of the present thiirane isotopologues Table 6 provides rotational constants for all fundamental bands. For comparison the high-resolution results of Bane *et al.* and Evans *et al.* [15, 16] are provided. Overall we find good agreement for rotational parameters with experimental values available. The corresponding MADs (in MHz) are 13, 21, and 12 for A_v, B_v, and C_v, respectively. The latter values agree with the deviations observed for the vibrational ground state (cf. Table 4). Therefore, the parameters which stand as predictions are assigned a conservative error of 30 MHz. Note that these results incorporate c-type Coriolis resonance corrections for the pairs ν_5/ν_{12} and ν_8/ν_{15}. These resonance were also confirmed experimentally [15, 16]. Additionally, an a-type Coriolis interaction is predicted between ν_3 and ν_7 ($\zeta^a_{3,7} = -0.419$). No experimental results are yet available for c-C_2D_4S and the presented constants stand as predictions. The H/D exchange does not change the occurence of Coriolis resonances in c-C_2D_4S, therefore an a-type resonance is predicted for the pair ν_3/ν_7 and c-type resonances for ν_5/ν_{12} and ν_8/ν_{15} ($\zeta^c_{8,15} = -0.796$). Based on the previous discussion the rotational constants for the deuterated isotopologue are also assigned a conservative error estimate of 30 MHz.

4. Summary and Conclusions

Thiirane and its fully deuterated isotopologue have been studied by high-level *ab initio* calculations. Multi-level multidimensional potential energy surfaces of coupled-cluster quality have been used to determine all fundamental transitions and low lying first overtones. Mean obsolute deviations of not more than 3.0 cm^{-1} were found with respect to various sets of experimental reference data. A number of misassignments could be resolved and a prediction of several vibrational overtones has been provided.

Rovibrational spectra for thiirane have been obtained from model Hamiltonian free RVCI theory and were compared with high-resolution spectra of Evans *et al.* [16] recorded using the far-IR beamline at the Australian synchrotron facility. The spectral range between 1400 and 1500 cm^{-1} has been studied for the first time. The spectra simulated for the deuterated species are predictions and need to be confirmed by new experiments.

Spectroscopic constants have been obtained from the polynomial fit of the PES within the framework of vibrational perturbation theory. Excellent agreement with experimental reference data based on Watson's A and S-reduced Hamiltonians has been found. The constants for the deuterated species are provided for the first time.

As a side aspect of this study, an expansion of the transition dipole moments within the framework of incremental vibrational configuration interaction theory has been implemented and was found to yield IR intensities of almost the same accuracy as obtained from standard configuration-selective VCI theory. This opens a new route for studying vibrational spectra exclusively by iVCI calculations.

The computational bottleneck of the presented calculations is given by the evaluation of the multidimensional PES, which took about 10 days on a customary workstation with 48 cores. The subsequent RVCI calculation took no longer than 6 hours on 10 cores. With that, the approach presented within this study can be used to study even larger molecules than thiirane.

Declaration of competing interest

The authors declare that they have no known competing financial interests or personal relationships that could have appeared to influence the research reported in this work.

Author contributions

John De Vos: Software, Formal analysis, Investigation, Writing - original draft, Writing - review & editing; **Benjamin Schröder**: Conceptualization, Methodology, Software, Supervision, Data Curation, Writing - original draft, Writing - review & editing; **Guntram Rauhut**: Supervision, Project administration, Conceptualization, Resources, Writing - original draft, Writing - review & editing, Funding acquisition.

Data Availability

The data that support the findings of this study, i.e. potential energy surfaces and line lists, are available online on the Zenodo database (https://www.doi.org/10.5281/zenodo.7781399).

Acknowledgements

The authors thank M. Tschöpe for help in preparing the figures. Financial support by the Deutsche Forschungsgemeinschaft (DFG), project Ra 656/29-1, is kindly acknowledged. BS acknowledges funding by the DFG (German Research Foundation) - 389479699/GRK2455, and JDV is grateful for financial support by the Research Foundation-Flanders (project no. 1163123N).

References

[1] C. Puzzarini, M. Biczysko, J. Bloino, V. Barone, Accurate spectroscopic characterization of oxirane: A valuable route to its identification in Titans's atmosphere and the assignment of unidentified infrared bands, Astrophys. J. 785 (2014) 1–8.

[2] C. Puzzarini, Astronomical complex organic molecules: Quantum chemistry meets rotational spectroscopy, Int. J. Quant. Chem. 117 (2017) 129–138.

[3] H. Thompson, D. Dupré, The infra-red and Raman spectra of ethylene sulphide, Trans. Faraday Soc. 36 (1940) 805–812.

[4] H. W. Thompson, W. T. Cave, The vibrational spectra of ethylene imine and ethylene sulphide, Trans. Faraday Soc. 47 (1951) 951–957.

Table 6: Computed and experimental[a] rotational constants (in MHz, I^r representation) for excited vibrational states of thiirane isotopologues.

	c-C_2H_4S			c-C_2D_4S		
v	A_v	B_v	C_v	A_v	B_v	C_v
ν_1	21915.10	10841.31	8033.43	15418.84	9203.79	6821.75
ν_2	21903.99	10853.85	8048.29	15376.82	9228.62	6827.39
ν_3	21819.89	10864.90	8030.45	15429.16	9219.78	6833.30
ν_4	21964.04	10863.63	8021.72	15485.82	9226.25	6810.63
	(21975.58)	(10843.70)	(8010.91)			
ν_5	21936.25	10803.19	8002.88	15447.71	9179.04	6802.63
	(21949.86)	(10782.67)	(7976.76)			
ν_6	21927.97	10842.74	8032.27	15438.53	9204.97	6817.84
ν_7	21881.56	10878.31	8057.66	15423.30	9249.85	6841.46
ν_8	21977.14	10811.93	8024.35	15483.05	9196.33	6816.83
	(21990.87)	(10790.08)	(8020.80)			
ν_9	21916.55	10840.86	8033.42	15427.65	9202.91	6821.76
ν_{10}	21927.61	10850.78	8049.50	15449.44	9219.20	6841.47
ν_{11}	21979.74	10830.47	8014.47	15476.53	9182.86	6804.39
	(21994.94)	(10809.62)	(8005.26)			
ν_{12}	22027.31	10767.53	7980.08	15478.92	9152.57	6788.05
	(22042.34)	(10745.52)	(7986.57)			
ν_{13}	21920.66	10844.72	8032.56	15429.02	9206.57	6818.05
ν_{14}	21984.05	10801.74	7999.86	15505.95	9180.60	6805.26
	(21993.10)	(10779.07)	(7989.65)			
ν_{15}	21895.43	10845.37	8031.33	15431.98	9215.20	6823.43
	(21907.21)	(10824.46)	(8016.64)			

[a] Experimental results in parentheses taken from Bane *et al.* [15] and Evans *et al.* [16].

[5] G. L. Cunningham Jr., A. W. Boyd, R. J. Myers, W. D. Gwinn, W. I. Le Van, The microwave spectra, structure, and dipole moments of ethylene oxide and ethylene sulfide, J. Chem. Phys. 19 (1951) 676–685.

[6] G. B. Guthrie Jr, D. W. Scott, G. Waddington, Thiacyclopropane (Ethylene Sulfide): Infrared Spectrum, Vapor Pressure and Some Thermodynamic Properties, J. Am. Chem. Soc. 74 (1952) 2795–2800.

[7] J. Lebrumant, Spectra of infrared absorption and Raman diffusion of solid thiethane, C. R. Acad. Sci. Paris 266 (1968) 1459.

[8] V. T. Aleksanyan, G. M. Kuz'yants, The vibrational spectra of thiirane, J. Struct. Chem. 12 (1971) 243–247.

[9] T. Hirokawa, M. Hayashi, H. Murata, Molecular vibrations and force constants of ethylene oxide, ethylene oxide-d_4, ethylene sulfide and ethylene sulfide-d_4, J. Sci. Hiroshima Univ., Ser A 37 (1973) 283–300.

[10] K. Okiye, C. Hirose, D. G. Lister, J. Sheridan, The r_s structure of ethylene sulphide, Chem. Phys. Lett. 24 (1974) 111–113.

[11] H. Hirose, K. Okiye, S. Maeda, The microwave spectrum of thiirane in excited vibrational states, Bull. Chem. Soc. Jpn 49 (1976) 916–921.

[12] W. D. Allen, J. E. Bertie, M. V. Falk, B. A. Hess, G. B. Mast, D. A. Othen, J. J. Schaad, H. F. Schaefer, The experimental vibrational spectra, vibrational assignment, and normal coordinate analysis of thiirane-h_4 and -d_4 and *cis*- and *trans*-1,2-dideuteriothiirane: *Ab initio* theoretical IR spectra of thiirane, thiirene, and isotopically substituted derivatives, J. Chem. Phys. 84 (1986) 4211–4227.

[13] B. Kirchner, H. Huber, G. Steinebrunner, H. Dreizler, J.-U. Grabow, I. Merke, Ab initio calculation of ^{33}S quadrupole coupling constants. Reanalysis of the ^{33}S hyperfine structure in the rotational spectrum of thiirane, Z. Naturforsch. 52a (1997) 297–305.

[14] T. Hirao, T. Okabayashi, M. Tanimoto, The r_0 structure of ethylene sulfide, J. Mol. Spectrosc. 208 (2001) 148–149.

[15] M. K. Bane, C. D. Thompson, D. R. T. Appadoo, D. McNaughton, Synchroton far infrared spectroscopy of the ground, ν_5 and ν_{15} states of thiirane, J. Chem. Phys. 137 (2012) 084306.

[16] C. J. Evans, J. P. Carter, D. R. T. Appadoo, A. Wong, D. McNaughton, Synchroton infrared spectroscopy of the ν_4, ν_8, ν_{10}, ν_{11} and ν_{14} fundamentals bands of thiirane, J. Mol. Spectrosc. 316 (2015) 32–37.

[17] J. E. Dickens, W. M. Irvine, M. Ohishi, M. Ikeda, S. Ishikawa, A. Nummelin, Å. Hjalmarson, Detection of Interstellar Ethylene Oxide (c-C_2H_4O), Astroph. J. 489 (1997) 753–757.

[18] D. P. Ruffle, T. W. Hartquist, P. Caselli, D. A. Williams, The sulphur depletion problem, Mon. Not. R. Astron. Soc. 306 (1999) 691–695.

[19] P. M. Woods, A. Occhiogrosso, S. Viti, Z. Kaňuchová, M. E. Palumbo, S. D. Price, A new study of an old sink of sulphur in hot molecular cores: the sulphur residue, Mon. Notices Royal Astron. Soc. 450 (2015) 1256–1267.

[20] R. Martín-Doménech, I. Jiménez-Serra, G. M. Muñoz Caro, H. S. P. Müller, A. Occhiogrosso, L. Testi, P. M. Woods, S. Viti, The sulfur depletion problem: upper limits on the H_2S_2, $HS_2^{\cdot}$, and S_2 gas-phase abundances toward the low-mass warm core IRAS 16293-2422, Astron. & Astrophys. 585 (2016) A112.

[21] D. V. Mifsud, Z. KaÅuchová, P. Herczku, S. Ioppolo, Z. Juhász, S. T. S. Kovács, N. J. Mason, R. W. McCullough, B. Sulik, Sulfur Ice Astrochemistry: A Review of Laboratory Studies, Space Sci. Rev. 217 (2021) 14.

[22] K. L. K. Lee, M.-A. Martin-Drumel, V. Lattanzi, B. A. McGuire, P. Caselli, M. C. McCarthy, Gas phase detection and rotational spectroscopy of ethynethiol, HCCSH, Mol. Phys. 117 (2019) 1381–1391.

[23] M.-A. Martin-Drumel, K. L. K. Lee, A. Belloche, O. Zingsheim, S. Thorwirth, H. S. P. Müller, F. Lewen, R. T. Garrod, K. M. Menten, M. C. McCarthy, S. Schlemmer, Submillimeter spectroscopy and astronomical searches of vinyl mercaptan, C_2H_3SH, Astron. & Astrophys. 623 (2019) A167.

[24] B. A. McGuire, C. N. Shingledecker, E. R. Willis, K. L. K. Lee, M.-A. Martin-Drumel, G. A. Blake, C. L. Brogan, A. M. Burkhardt, P. Caselli, K.-J. Chuang, S. El-Abd, T. R. Hunter, S. Ioppolo, H. Linnartz, A. J. Remijan, C. Xue, M. C. McCarthy, Searches for Interstellar HCCSH and H_2CCS, Astrophys. J. 883 (2019) 201.

[25] H. H. Nielsen, The Vibration-rotation Energies of Molecules and their Spectra in the Infra-red, in: S. Flügge (Ed.), Handbuch der Physik, Vol. 37, Part I, Springer, Berlin, 1959, pp. 173–313.

[26] G. Amat, H. H. Nielsen, , G. Tarrago, Rotation-Vibration of Polyatomic Molecules, Dekker, New York, 1971.

[27] D. Papoušek, M. R. Aliev, Molecular Vibrational-rotational Spectra: Theory and Applications of High Resolution Infrared, Microwave and Raman Spectroscopy of Polyatomic Molecules, Elsevier Science Ltd, 1982.

[28] M. R. Aliev, J. K. G. Watson, Higher-order effects in the vibration-rotation spectra of semirigid molecules, in: K. N. Rao (Ed.), Molecular Spectroscopy: Modern Research, Academic Press, 1985, pp. 1–67.

[29] D. A. Clabo, W. D. Allen, R. B. Remington, Y. Yamaguchi, H. F. Schaefer, A systematic study of molecular vibrational anharmonicity and vibration-rotation interaction by self-consistent-field higher-derivative methods - Asymmetric-top molecules, Chem. Phys. 123 (1988) 187–239.

[30] M. Piccardo, J. Bloino, V. Barone, Generalized vibrational perturbation theory for rotovibrational energies of linear, symmetric and asymmetric tops: Theory, approximations, and automated approaches to deal with medium-to-large molecular systems, Int. J. Quant. Chem. 115 (2015) 948–982.

[31] C. Puzzarini, J. Bloino, N. Tasinato, V. Barone, Accuracy and Interpretability: The Devil and the Holy Grail. New Routes across Old Boundaries in Computational Spectroscopy, Chem. Rev. 119 (2019) 8131–8191.

[32] V. Barone, S. Alessandrini, M. Biczysko, J. R. Cheeseman, D. C. Clary, A. B. McCoy, R. J. DiRisio, F. Neese, M. Melosso, C. Puzzarini, Computational molecular spectroscopy, Nat. Rev. Methods Primers 1 (2021).

[33] S. Califano, Vibrational States, John Wiley & Sons, Inc., London, 1976.

[34] S. V. Krasnoshchekov, E. V. Isayeva, N. F. Stepanov, Criteria for first- and second-order vibrational resonances and correct evaluation of the Darling-Dennison resonance coefficients using the canonical Van Vleck perturbation theory, J. Chem. Phys. 141 (2014) 234114.

[35] S. V. Krasnoshchekov, E. O. Dobrolyubov, M. A. Syzgantseva, R. V. Palvelev, Rigorous vibrational fermi

resonance criterion revealed: two different approaches yield the same result, Mol. Phys. 118 (2020) e1743887.

[36] J. M. L. Martin, T. J. Lee, P. R. Taylor, J. François, The anharmonic force field of ethylene, C_2H_4, by means of accurate *ab initio* calculations, J. Chem. Phys. 103 (1995) 2589–2602.

[37] J. L. Davisson, N. R. Brinkmann, W. F. Polik, Accurate and efficient calculation of excited vibrational states from quartic potential energy surfaces, Mol. Phys. 110 (2012) 2587–2598.

[38] A. M. Rosnik, W. F. Polik, VPT2+K spectroscopic constants and matrix elements of the transformed vibrational Hamiltonian of a polyatomic molecule with resonances using Van Vleck perturbation theory, Mol. Phys. 112 (2014) 261–300.

[39] P. R. Franke, J. F. Stanton, G. E. Douberly, How to VPT2: Accurate and Intuitive Simulations of CH Stretching Infrared Spectra Using VPT2+K with Large Effective Hamiltonian Resonance Treatments, J. Phys. Chem. A 125 (2021) 1301–1324.

[40] Q. Yang, J. Bloino, An Effective and Automated Processing of Resonances in Vibrational Perturbation Theory Applied to Spectroscopy, J. Phys. Chem. A 126 (2022) 9276–9302.

[41] M. A. Boyer, A. B. McCoy, A wave function correction-based approach to the identification of resonances for vibrational perturbation theory, J. Chem. Phys. 157 (2022) 164113.

[42] J. M. Bowman, T. Carrington Jr., H. D. Meyer, Variational quantum approaches for computing vibrational energies of polyatomic molecules, Mol. Phys. 106 (2008) 2145–2182.

[43] B. Schröder, G. Rauhut, Vibrational configuration interaction theory, World Scientific Publishing, Singapore, 2022, Ch. 1, pp. 1–40.

[44] B. Schröder, G. Rauhut, Incremental vibrational configuration interaction theory, iVCI: Implementation and benchmark calculations, J. Chem. Phys. 154 (2021) 124114.

[45] B. Schröder, G. Rauhut, Comparison of body definitions for incremental vibrational configuration interaction theory (iVCI), J. Chem. Phys. 156 (2022) 174103.

[46] S. Erfort, M. Tschöpe, G. Rauhut, Toward a fully automated calculation of rovibrational infrared intensities for semi-rigid polyatomic molecules, J. Chem. Phys. 152 (2020) 244104.

[47] S. Erfort, M. Tschöpe, G. Rauhut, Efficient and automated quantum chemical calculation of rovibrational nonresonant Raman spectra, J. Chem. Phys. 156 (2022) 124102.

[48] J. K. G. Watson, Simplification of the molecular vibration-rotation Hamiltonian, Mol. Phys. 15 (1968) 479–490.

[49] M. Tschöpe, G. Rauhut, Convergence of series expansions in rovibrational configuration interaction (RVCI) calculations, J. Chem. Phys. 157 (2022) 234105.

[50] T. B. Adler, G. Knizia, H.-J. Werner, A simple and efficient CCSD(T)-F12 approximation, J. Chem. Phys. 127 (2007) 221106.

[51] J. G. Hill, S. Mazumder, K. A. Peterson, Correlation consistent basis sets for molecular core-valence effects with explicitly correlated wave functions: the atoms B-Ne and Al-Ar, J. Chem. Phys. 132 (2010) 054108.

[52] F. Weigend, A fully direct ri-hf algorithm: Implementation, optimised auxiliary basis sets, demonstration of accuracy and efficiency, Phys. Chem. Chem. Phys. 4 (2002) 4285–4291.

[53] F. Weigend, A. Köhn, C. Hättig, Efficient use of the correlation consistent basis sets in resolution of the identity MP2 calculations, The Journal of Chemical Physics 116 (8) (2002) 3175–3183.

[54] C. Hättig, Optimization of auxiliary basis sets for RI-MP2 and RI-CC2 calculations: Core–valence and quintuple-ζ basis sets for H to Ar and QZVPP basis sets for Li to Kr, Phys. Chem. Chem. Phys. 7 (2005) 59–66.

[55] H.-J. Werner, G. Knizia, F. R. Manby, Explicitly correlated coupled cluster methods with pair-specific geminals, Mol. Phys. 109 (2011) 407–417.

[56] G. Knizia, H.-J. Werner, Explicitly correlated RMP2 for high-spin open-shell reference states, J.Chem. Phys. 128 (2008) 15410.

[57] K. Pflüger, M. Paulus, S. Jagiella, T. Burkert, G. Rauhut, Multi-level vibrational SCF calculations and FTIR measurements on furazan, Theor. Chem. Acc. 114 (2005) 327–332.

[58] D. Kats, F. R. Manby, Communication: The distinguishable cluster approximation, J. Chem. Phys. 139 (2013) 021102.

[59] T. H. Dunning, Gaussian basis sets for use in correlated molecular calculations. I. The atoms boron through neon and hydrogen, J. Chem. Phys. 90 (2) (1989) 1007–1023.

[60] D. E. Woon, T. H. Dunning, Gaussian basis sets for use in correlated molecular calculations. III. The atoms aluminum through argon, J. Chem. Phys. 98 (2) (1993) 1358–1371.

[61] B. Ziegler, G. Rauhut, Efficient generation of sum-of-products representations of high-dimensional potential energy surfaces based on multimode expansions, J. Chem. Phys. 144 (2016) 114114.

[62] J. M. Bowman, Self-consistent field energies and wavefunctions for coupled oscillators, J. Chem. Phys. 68 (1978) 608–610.

[63] G. Rauhut, Efficient calculation of potential energy surfaces for the generation of vibrational wave functions, J. Chem. Phys. 121 (2004) 9313–9322.

[64] T. Mathea, G. Rauhut, Advances in vibrational configuration interaction theory - part 1: Efficient calculation of vibrational angular momentum terms, J. Comp. Chem. 42 (2021) 2321–2333.

[65] T. Mathea, T. Petrenko, G. Rauhut, Advances in vibrational configuration interaction theory - part 2: Fast screening of the correlation space, J. Comp. Chem. 43 (2022) 6–18.

[66] H.-J. Werner, P. J. Knowles, F. R. Manby, J. A. Black, K. Doll, A. Heßelmann, D. Kats, A. Köhn, T. Korona, D. A. Kreplin, Q. Ma, T. F. Miller, A. Mitrushchenkov, K. A. Peterson, I. Polyak, G. Rauhut, M. Sibaev, The Molpro quantum chemistry package, J. Chem. Phys. 152 (2020) 144107.

[67] G. Czakó, E. Mátyus, A. G. Császár, Bridging Theory with Experiment: A Benchmark Study of Thermally Averaged Structural and Effective Spectroscopic Parameters of the Water Molecule, J. Phys. Chem. A 113 (43) (2009) 11665 – 11678.

[68] D. F. Dinu, B. Ziegler, M. Podewitz, K. R. Liedl, T. Loerting, H. Grothe, G. Rauhut, The interplay of VSCF/VCI calculations and matrix-isolation IR spectroscopy – Mid infrared spectrum of CH_3CH_2F and

CD_3CD_2F, J. Mol. Spectrosc. 367 (2020) 111224.

[69] M. Spiekermann, D. Bougeard, B. Schrader, Coupled calculations of vibrational frequencies and intensities. III. IR and Raman spectra of ethylene oxide and ethylene sulfide, J. Comput. Chem. 3 (1982) 354–362.

[70] J. K. G. Watson, Centrifugal corrections for asymmetric-top molecules, J. Chem. Phys. 45 (1966) 1360–1361.

[71] J. K. G. Watson, Determination of centrifugal-distortion coefficients of asymmetric-top molecules, J. Chem. Phys. 46 (1967) 1935–1949.

[72] J. K. G. Watson, Determination of centrifugal-distortion coefficients of asymmetric top molecules. II. Dreizler, Dendl, and Rudolph's results, J. Chem. Phys. 48 (1968) 181–185.

[73] J. K. G. Watson, Determination of centrifugal distortion coefficients of asymmetric top molecules. III. Sextic coefficients, J. Chem. Phys. 48 (1968) 4517–4524.

[74] R. Ramakrishnan, G. Rauhut, Semi-quartic force fields retrieved from multi-mode expansions: Accuracy, scaling behavior, and approximations, J. Chem. Phys. 142 (2015) 154118.